DOI 10.1007/s11182-015-0422-z

Russian Physics Journal, Vol. 57, No. 11, March, 2015 (Russian Original No. 11, November, 2014)

PHYSICS OF SEMICONDUCTORS AND DIELECTRICS

MEASUREMENT OF THE CHARGE CARRIER MOBILITY IN MEH-PPV AND MEH-PPV-POSS ORGANIC SEMICONDUCTOR FILMS

I. V. Romanov, A. V. Voitsekhovskii, K. M. Dyagterenko, T. N. Kopylova, A. P. Kokhanenko, and E. N. Nikonova

UDC 535.37; 537.31

The values of the charge carrier mobility in organic semiconductor materials (MEH-PPV, MEH-PPV-POSS) are obtained on the basis of an analysis of the relaxation curves of transient electroluminescence in organic light-emitting diodes (OLEDs). The data on the mobility of charge carriers are analyzed according to the Poole–Frenkel model using the dependences of the charge carrier mobility on the electric field. Physical interpretation of the transport phenomena in OLED structures based on MEH-PPV and MEH-PPV-POSS is given.

Keywords: organic semiconductors, thin polymer films, OLED, charge carrier mobility, measurement techniques, electroluminescence, MEH-PPV, MEH-PPV-POSS.

Currently, optoelectronic devices based on organic semiconductors are manufactured. OLEDs and photodetectors (PD) are being actively implemented in the data transmission technology using polymer waveguides. For example, [1] presents the results on the data transmission via polymer optical waveguides, where organic devices are used as a source and a recorder of an optical signal. In [2], organic light-emitting diodes operating in the high-speed optical communication networks are studied. The low cost and relative ease of manufacturing techniques of these electroluminescent devices [3] allowed in a short time to create effective OLEDs and flat widescreen displays. However, low mobility of charge carriers in organic semiconductors limits the performance of devices based on these materials [4]. Thus, the mobility and radiative lifetime of charge carriers are, along with the quantum efficiency, important factors responsible for the brightness and performance of OLEDs and photodetectors. Performance of an organic light-emitting diode is determined by the structure and electrical and recombination parameters of organic materials, the diode is based on. The shorter the time required for the carrier passage from the electrodes into the emission region, the higher the performance of the light-emitting diode. Therefore, determination of the charge carrier mobility is necessary for the development of high-performance organic light-emitting diodes.

To measure the charge carrier mobility in organic semiconductors, several methods are used: a time-of-flight method (TOF), a radiation-induced variant of the time-of-flight method, a method of extraction of charge carriers by a linearly increasing field, and the transient electroluminescence method (TEL). Each of these methods has its own advantages and disadvantages. For example, it is believed that the time-of-flight method allows most accurately to determine the mobility of charge carriers. Main difficulty in application of this method is that the layer thickness of the measured material should be about 4–10 μm. The thickness of organic light emitting diodes used in practice is about

National Research Tomsk State University, Tomsk, Russia, e-mail: drsuvar@gmail.com. Translated from Izvestiya Vysshikh Uchebnykh Zavedenii, Fizika, No. 11, pp. 116–123, November, 2014. Original article submitted May 12, 2014.

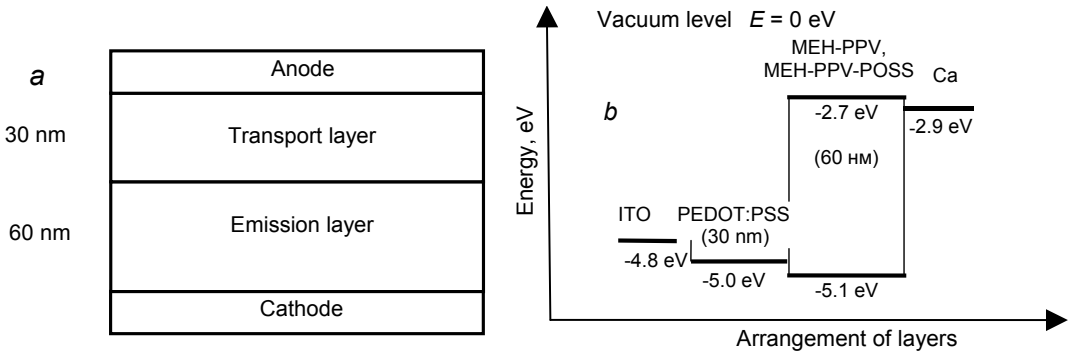

Fig. 1. Structure (*a*) and energy diagram (*b*) of OLED layers.

100 nm, which makes this method inapplicable for most of OLEDs, whose layer thickness is less than one micrometer. The most suitable method for measuring the mobility in these layers is the method of transient electroluminescence. This method also provides a possibility to measure the mobility of both majority and minority charge carriers in organic semiconductor layers of submicron thicknesses.

Our research is focused on testing the method of the surface electroluminescence for the determining the charge carrier mobility in thin films of MEH-PPV and MEH-PPV-POSS, which are the basic materials for OLEDs [5]. The number and composition of layers determine the energy efficiency of electroluminescence. To obtain the accurate values of the charge carrier mobility in an active layer of LED, it is desirable to use a three-layer structure (an anode – an emission layer – a cathode). In practice, in such a structure, it is not always possible to obtain the electroluminescence intensity acceptable for measurements, which hampers the electroluminescence registration in the presence of the measuring circuit noise and background. This results in an increase in the error of the charge carriers mobility measurement at low values of the electric field applied to the structure contacts. Introduction of the transport layers can increase the light flux of OLEDs and reduce the operating voltages. The objects of the study are the organic light emitting devices, whose energy levels are shown in Fig. 1.

The OLED samples had the following structure: a glass substrate – an anode – a *p*-type transport layer – an emission layer – a cathode – a glass substrate (Fig. 1*a*). The anode is a layer of ITO – indium tin oxide (In_2O_3:SnO_2). The transport and emission layers were deposited by centrifugation from the aqueous and toluene solutions, respectively. The transport layer allows to improve the hole injection from the anode and to provide the balance between the electron and hole currents preventing the transit of carriers through the OLED structure. The cathode consists of a layer of calcium coated by an aluminum protective layer. The metal layers are deposited sequentially by thermal spraying of metal in the vacuum. The anode and cathode inject holes and electrons, respectively. Measurement of the hole mobility in the emission layer was carried out with the following substances: poly (2-methoxy-5-(2'-ethylhexyloxy)-1,4-phenylenevinylene (MEH-PPV), poly (2-metoxy-5-(2'-ethylhexyloxy)-1,4-phenylenevinylene with adjoint polyhedral oligomeric silsesquioxane (MEH-PPV-POSS). As a *p*-type transport layer, the PEDOT:PSS (poly (3,4-ethylene dioxythiophene): poly (styrene sulfonate)) was used. It was found that the electroluminescence spectrum of the sample has a maximum at a wavelength of 598 nm.

Figure 2*a* shows the experimental setup for the recording the transient electroluminescence in the OLED samples, where FEU is the photoelectron multiplier. Figure 2*b* shows the transient electroluminescence signal of OLEDs at the anode – cathode voltage of 10 V and the smoothing curve of this signal.

To apply the rectangular voltage pulses to the OLED samples, a pulse generator was used. The rise and fall times of pulses of this generator were not more than 10 ns. The amplitude of pulses at the output of the generator may vary in the range from 0 to 11 V. Measurements of the transient electroluminescence of OLEDs were performed at room temperature. Electroluminescence of OLEDs was recorded by a photomultiplier with the sensitivity range 300–600 nm. At the output of the photomultiplier, the photosignal amplitude is from few to few tens of millivolts (see Fig. 2*a*), depending on the electroluminescence intensity in OLEDs. The photosignal from the photomultiplier is supplied to the input of an amplifier with an adjustable gain (10-20 dB). From the output of the amplifier, the

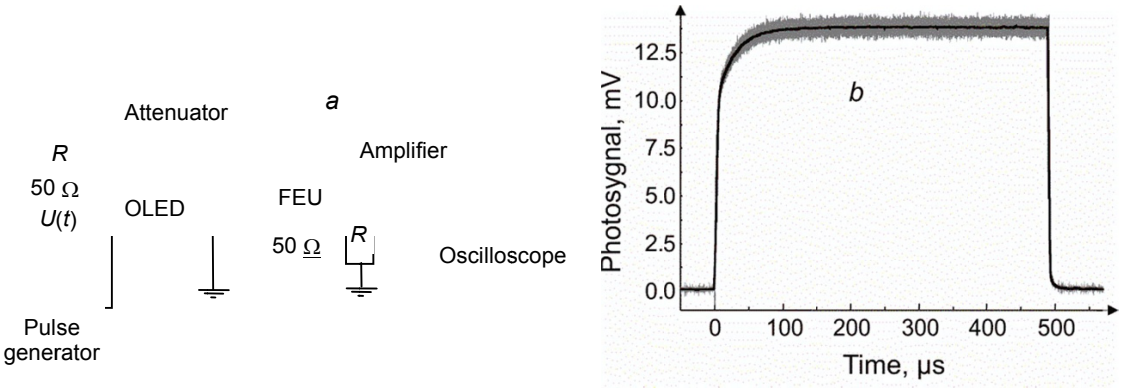

Fig. 2. Experimental setup for the measurements of transient electroluminescence (*a*) and the transient electroluminescence signal at the anode – cathode voltage of 10 V (*b*).

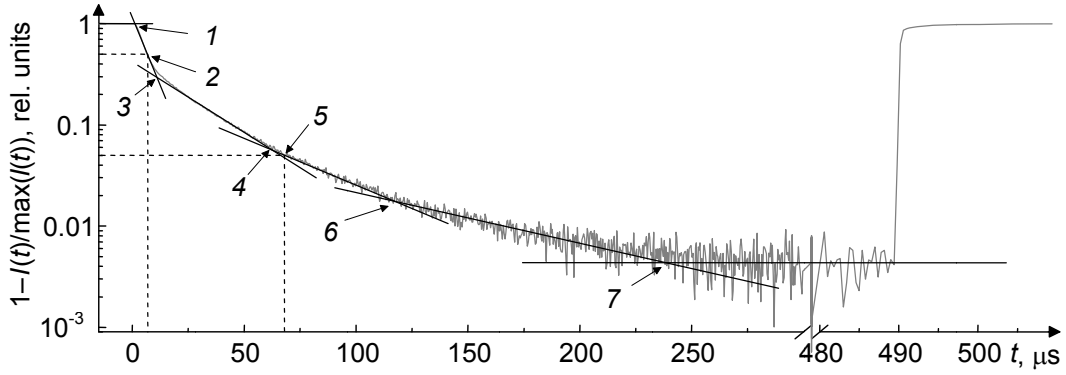

Fig. 3. The relaxation curve of the normalized transient electroluminescence intensity in different scales: *1* – the delay time of holes ($t_{d,h}$), *2* – the transit time of holes at the 0.5 level ($t_{0.5}$), *3* – the transit time of holes ($t_{tr,h}$), *4* – the delay time of electrons ($t_{d,e}$), *5* – the delay time of electrons at the 0.95 level ($t_{0.95}$), *6* – the transit time of electrons ($t_{tr,e}$), and *7* – the time of establishing of the stationary intensity of OLEDs.

photosignal is supplied to the input of a digital oscilloscope (LeCroy WS 62), where it is recorded. The characteristic RC time constant in the measuring circuit does not exceed 1 μs.

If voltage is applied to the OLED, a number of charged particles coming to the contact will vary with time and depend on the properties of organic semiconductors comprising the OLED. Figure 3 shows the normalized intensity of the transient electroluminescence $I(t)$. The intersection points of the asymptotic lines in Fig. 3 correspond to the delay times t_d and transit times t_{tr} of charge carriers (electrons and holes) in the OLED emission layer (Fig. 4). The delay time is the time that a charged particle (an electron or a hole) requires to overcome the distance between the anode and cathode. It is assumed that the delay time characterizes the most rapid part of the charged particle flight. The time, at which most of charge carriers arrive to the OLED contacts, is called the transit time.

The value of $t_{d,h}$ (*1* in Fig. 3) corresponds to the arrival of "fast" holes from the anode to the cathode. In this case, at the emission layer–cathode interface, the hole and electron fluxes meet together to form excitons (the recombination takes place). Then, the excitons decay with emission of light. Let us call the region in the emission layer, where the generation of light takes place, an active region. The value of $t_{tr,h}$ (*3* in Fig. 3) corresponds to the arrival of the main ("slow") part of holes from the anode to the cathode. At $t_{tr,h}$, d_3 is less than d_1.

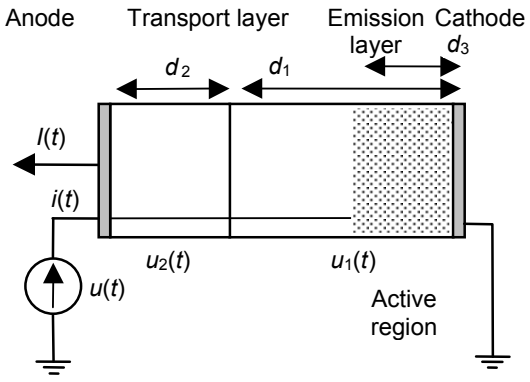

Fig. 4. Wiring diagram and the structure of OLEDs.

Here, d_1, d_2, and d_3 are the thicknesses of the emission layer, transport layer, and active region, respectively. The value of $t_{d,e}$ (*4* in Fig. 3) describes the arrival of "fast" electrons from the cathode to the transport layer–emission layer interface. Thus, an active region (a light generation region) is increased. The value of $t_{tr,e}$ (*6* in Fig. 3) describes the arrival of the main ("slow") part of electrons from the cathode to the transport layer–emission layer interface. At $t_{tr,e}$, the active region thickness (d_3 in Fig. 4) becomes close to the emission layer thickness (d_1 in Fig. 4).

It is interesting to consider the mobility of charge carriers in the emission layer. As stated above, in an organic semiconductor, holes and electrons move with different speeds. Analyzing the leading edge of the pulse of the electroluminescence of OLEDs, we can distinguish the "fast» μ_d and "slow» μ_{tr} holes and electrons. The mobilities of these charge carriers in the emission layer of an OLED can be defined by the following expressions:

$$\mu_{d,h} = \frac{d_1}{E \cdot t_{d,h}},\ \mu_{0.5} = \frac{d_1}{E \cdot t_{0.5}},\ \mu_{tr,h} = \frac{d_1}{E \cdot t_{tr,h}},$$

$$\mu_{d,e} = \frac{d_1}{E \cdot t_{d,e}},\ \mu_{0.95} = \frac{d_1}{E \cdot t_{0.95}},\ \mu_{tr,e} = \frac{d_1}{E \cdot t_{tr,e}}. \quad (1)$$

Here E is the electric field strength in the emission layer of an OLED. The characteristic times $t_{0.5}$ and $t_{0.95}$ allow to approximately estimate the hole and electron mobilities in the case, where the values of $t_{d,h}$, $t_{tr,h}$, $t_{d,e}$, and $t_{tr,e}$ cannot be determined in the experiment.

To simplify the notation, we denote the sets of variables as $\{t_{d,h}, t_{0.5}, t_{tr,h}, t_{d,e}, t_{0.95}, t_{tr,e}\} = t_*$ and $\{\mu_{d,h}, \mu_{0.5}, \mu_{tr,h}, \mu_{d,e}, \mu_{0.95}, \mu_{tr,e}\} = \mu_*$. Then, Eq. (1) can be rewritten as

$$\mu_* = \frac{d_1}{E \cdot t_*}, \quad (2)$$

where t_* is the characteristic delay/transit time of carriers through the emission layer and μ_* is a typical charge carrier mobility in the emission layer.

To find the mobility of these charge carriers, we need to make some assumptions about the properties of the OLED layers. The voltage u is applied to the contacts of the structure and the current i flows through the OLED. The voltage drop in the structure is distributed between the layers. In the stationary approximation, the Ohm's law requires the fulfillment of the expressions

$$i = i_1 = i_2, \quad (3)$$

$$u = u_1 + u_2 = \frac{i_1 \cdot d_1}{S \cdot \sigma_1} + \frac{i_2 \cdot d_2}{S \cdot \sigma_2}, \tag{4}$$

where u, u_1, and u_2 are the total voltage drops in the anode – cathode contacts of an OLED, in the emission layer, and in the transport layer, respectively, i, i_1, i_2 are the electric currents flowing through the OLED, in the emission layer, and in the transport layer, respectively, σ_1 and σ_2 are the specific conductivities of the emission and transport layers, respectively. The specific conductivity of the transport layer σ_2 (in our case, PEDOT:PSS) is much higher, than the specific conductivities of the emission layer σ_1 (MEH-PPV). Therefore, the second term in Eq. (4) can be neglected, and we can assume that the whole voltage applied to the structure drops in the emission layer $u_1 \cong u$.

Then, the electric field strength in the emission layer of the OLED (in the absence of the space charge) can be determined by the following expression:

$$E = \frac{u - u_{bi}}{d_1 + d_2}, \tag{5}$$

where u_{bi} is the built-in voltage of the OLED [5].

On the example of an OLED with the structure shown in Fig. 4, we define the necessary conditions, at which the introduction of the transport layer into the OLED will not affect the accuracy of determining the mobility of charge carriers in the emission layer. To eliminate the influence of the delay/transit processes of charge carriers in the transport layer (t_2) on the measurement results of the delay/transit time of charge carriers in the emission layer (t_1), we should select the materials of transport layers, where the mobility of charge carriers is much greater, than the charge carrier mobility in the emission layer. Then the delay/transit times of charge carriers through the transport layers can be neglected, ie, $t_1 + t_2 \approx t_1 = t_*$.

Under the influence of an electric field applied to the OLED contacts, electrons injected from the cathode move toward the anode (Fig. 4). Since the mobility of electrons in the emission layer is much smaller than the mobility of holes, the time of arrival of electrons to the transport layer–emission layer interface is much greater, than the transit time of holes between the anode and cathode. Electrons that overcome the transport layer–emission layer interface, are not involved in the process of radiative recombination. This leads to the fact that the delay times $t_{d,e}$ and the transit times $t_{tr,e}$ characterize the electron transport in the emission layer. Therefore, in the calculation formulas of the electron mobility in a multilayer OLED, the delay of electrons in the transport layer can be disregarded.

Then, with regard to (2) and (5), the charge carrier mobility in the emission layer can be written as

$$\mu_* = \frac{d_1 \cdot (d_1 + d_2)}{(u - u_{bi}) \cdot t_*}. \tag{6}$$

The delay and transit times t_* are determined as described in [5-7] using the intersection of the asymptotic straight lines (the lines in Fig. 3).

There are several experimental methods to determine the built-in voltage u_{bi}: a method of capacitance-voltage measurements [8], photovoltaic measurements [9], current-voltage measurements [10], and an electroabsorption method [11, 12]. In our study, we restrict ourselves by the method of an analysis of the energy diagram of OLED (see. Fig. 1*a*) [13]. An expression connecting the built-in voltage u_{bi}, the band gap of the semiconductor E_g, the hole Φ_h and electron Φ_e injection barriers for the anode and cathode, respectively, can be written as $\Phi_h + \Phi_e = E_g - u_{bi}/q$. Taking into account the energy diagram of the OLED (Fig. 1), u_{bi} is approximately equal to 1.9 V.

Figure 5 shows the dependence of the electric current i flowing through the sample, when the constant voltage u is applied to the contacts of the OLED (Fig. 1). From the current-voltage dependence constructed in the double logarithmic scale at voltages u from 0.1 to 8 V, two characteristic regions can be exactly determined. The first region is located in the voltage range $0 < u < 2.3$ V. Here, the current is limited by the resistance of the semiconductor layer in the absence of the charge carrier injection from the OLED contacts. The second region is located at voltages $u > 2.3$ V.

Formulas for the electric current flowing through the sample can be written as follows: [5]:

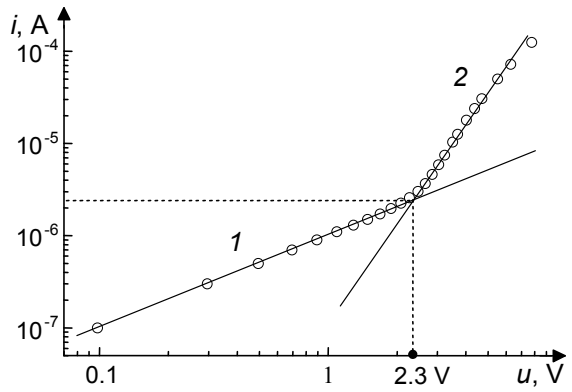

Fig. 5. Current-voltage characteristic of an OLED sample.

$$i_{ohm} = n_0 q \mu S \frac{(u - u_{bi})}{d_1}, \tag{7}$$

$$i_{scl} = \frac{9}{8} \varepsilon \varepsilon_0 \mu S \frac{(u - u_{bi})^2}{d_1^3}. \tag{8}$$

Here, n_0 is the intrinsic concentration of charge carriers in the semiconductor layer, q is an elementary electrical charge, μ is the effective mobility of carriers in the semiconductor (if $\mu_h >> \mu_e$, $\mu \cong \mu_h$), d_1 is the semiconductor layer thickness, S is the area, ε is the permittivity of the semiconductor, and ε_0 is the permittivity of vacuum. These expressions correspond to the ohmic current component (7) and current component limited by the space charge. That is, at high voltages, the current-voltage characteristic $i(u)$ is not described by the Ohm's law, but it has the injection nature. The mode of the OLED operation depends on the values of the operating voltages. The critical voltage value (the inflection point in the dependence $i(u)$ in Fig. 5) is

$$u_{\text{cr}} = \frac{8}{9} \frac{q}{\varepsilon \varepsilon_0} n_0 d_1^2. \tag{9}$$

From Eq. (9), we can find the hole concentration assuming that the permittivity ε of MEH-PPV is equal to 3 and that the value of u_{cr} corresponding to the point of transition from the ohmic to the space-charge limitation of current in the OLED is equal to $2.3 - u_{bi} = 0.4$ V. Then, the concentration of holes in the emission layer MEH-PPV is $n_0 \simeq 2 \cdot 10^{16}$ cm^{-3}. An effective mobility of charge carriers in the sections of the current-voltage characteristic can be obtained from (8):

$$\mu = \frac{8}{9} \frac{i_{scl} d_1^3}{\varepsilon \varepsilon_0 S (u - u_{bi})^2}. \tag{10}$$

Calculation using Eq. (10) at $u_{\text{cr}} = 0.4$ V gives the following value of an effective mobility: $\mu = 1.82 \cdot 10^{-7}$ cm$^2 \cdot$V$^{-1} \cdot$s^{-1}.

Experiments were performed on the OLED samples fabricated on the substrate with the lithographic profiling of ITO layer and with the solid cathode (Fig. 6). The area of an active region in the OLED samples was 6 mm^2. The mobility measurements were conducted at six pixels on the OLED samples with the structures ITO/PEDOT:PSS/MEH-PPV/Ca/Al and ITO/PEDOT:PSS/MEH-PPV-POSS/Ca/Al (see. Figs. 1 and 4).

Figure 7 shows the results of measurements of the field dependences of the hole and electron mobility in the emission layer of the OLED samples based on the two materials: MEH-PPV (*a*) and MEH-PPV-POSS (*b*).

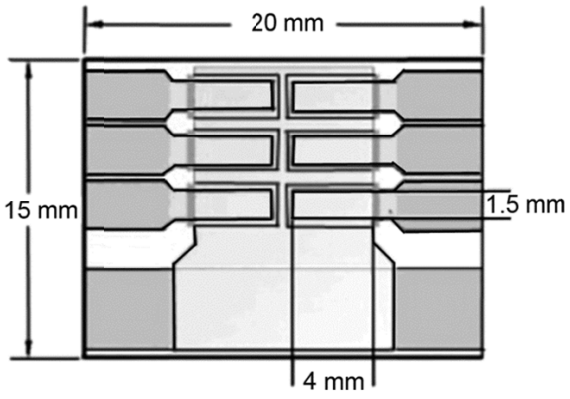

Fig. 6. Lithographic profile of OLED samples.

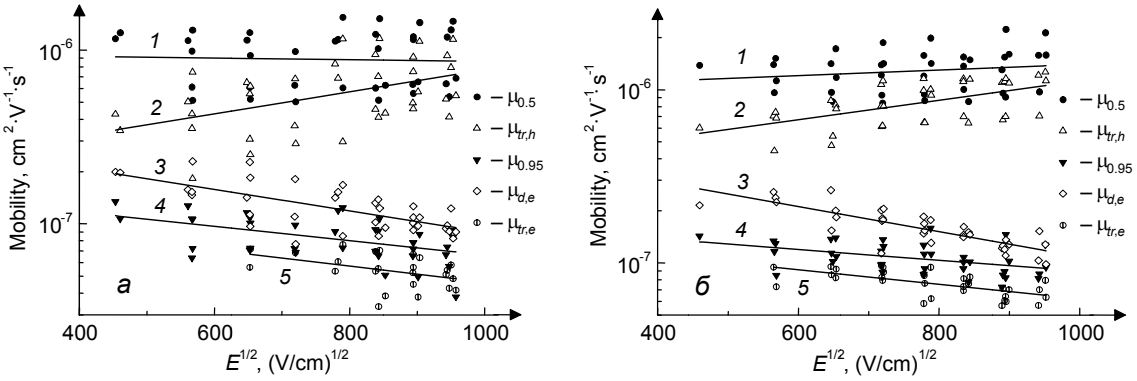

Fig. 7. Mobilities of holes and electrons in the emission layer of MEH-PPV (*a*) and MEH-PPV-POSS (*b*): *1* – hole mobility $\mu_{0.5}$ (at the 0.5 level), *2* – hole mobility $\mu_{tr,h}$, *3* – electron mobility $\mu_{d,e}$, *4* – electron mobility $\mu_{0.95}$ (at the 0.95 level), *5* – electron mobility $\mu_{tr,e}$.

An advantage of studies of the mobility in the OLED samples at six pixels is the possibility to obtain the more accurate values of the mobility due to theirs averaging.

The measured hole mobilities in the emission layer of OLED are consistent with the data published by other researchers for the MEH-PPV and MEH-PPV-POSS [14, 15]. The mobilities in Fig. 7 are constructed as a function of the square root of the electric field strength applied to the sample, since, for the organic materials, according to the Poole–Frenkel model, the dependence of the mobility on the electric field strength at a fixed temperature must satisfy the expression [16]

$$\mu(E) = \mu_0 \cdot \exp\left(\frac{\beta_{P-F} E^{\frac{1}{2}}}{kT}\right),$$

where μ_0 is the charge carrier mobility in the absence of electric field and β_{P-F} is the constant coefficient. By extrapolating the data presented in Fig. 7, the hole mobilities in the absence of an applied field (initial mobility) $\mu_*(0)$ were calculated for the MEH-PPV and MEH-PPV-POSS. The coefficient β_{P-F} is defined as the slope in the coordinates $\ln(\mu_*) - E^{1/2}$. The values of β_{P-F} were determined from the plots shown in Fig. 7.

TABLE 1. Values of an Initial Charge Carrier Mobility and the Coefficient of Poole–Frenkel

Mobility	MEH-PPV		MEH-PPV-POSS	
	$\mu_*(0)$, $cm^2 \cdot V^{-1} \cdot s^{-1}$	β_{P-F}, $eV(cm/V)^{1/2}$	$\mu_*(0)$, $cm^2 \cdot V^{-1} \cdot s^{-1}$	β_{P-F}, $eV(cm/V)^{1/2}$
$\mu_{d,h}$	–	–	–	–
$\mu_{0.5}$	$9.6 \cdot 10^{-7}$	$-2.7 \cdot 10^{-6}$	$9.6 \cdot 10^{-7}$	$9.4 \cdot 10^{-6}$
$\mu_{tr,h}$	$1.8 \cdot 10^{-7}$	$3.7 \cdot 10^{-5}$	$3.1 \cdot 10^{-7}$	$3.3 \cdot 10^{-5}$
$\mu_{d,e}$	$3.7 \cdot 10^{-7}$	$-3.6 \cdot 10^{-5}$	$5.7 \cdot 10^{-7}$	$-4.2 \cdot 10^{-5}$
$\mu_{0.95}$	$1.7 \cdot 10^{-7}$	$-2.4 \cdot 10^{-5}$	$1.8 \cdot 10^{-7}$	$-1.8 \cdot 10^{-5}$
$\mu_{tr,e}$	$1.3 \cdot 10^{-7}$	$-2.7 \cdot 10^{-5}$	$1.6 \cdot 10^{-7}$	$-2.4 \cdot 10^{-5}$

During the experimental measurements of the transient electroluminescence of OLED samples based on MEH-PPV and MEH-PPV-POSS, we failed in measuring the delay time of holes $t_{d,h}$ because of the background light. Therefore, in Table 1, there are no values of $\mu_{d,h}$.

Thus, the field dependences of the drift electron and hole mobilities in the emission layer of organic light-emitting diodes based on the two organic semiconductors MEH-PPV and MEH-PPV-POSS are experimentally measured. The values of the hole and electron mobility in the absence of an applied field are determined for the two organic semiconductors MEH-PPV and MEH-PPV-POSS. For these semiconductors, the coefficients β_{P-F}, are also determined. The measurement results (Table I) show that an addition of the polyhedral oligomeric silseskioksan to the poly(2-methoxy-5-(2'-ethylhexyloxy)-1,4-fenilenvinilen does not substantially affect the nature of the charge carrier transport in the emission layer of the OLED. The difference in the values of the charge carrier mobilities (Fig. 7*a*, *b*, and Table 1) can be explained by the error in the determination of the OLED sample sizes. We note that in OLEDs, the hole mobility increases and the electron mobility decreases with increasing electric field strength.

The values of the concentration n_0 and effective hole mobility are theoretically calculated at a critical value of the voltage u_{cr} on the contacts of an OLED based on the organic semiconductor MEH-PPV. The fact that experimental values of $\mu_{tr,h}(0) = 1.8 \cdot 10^{-7}$ $cm^2 \cdot V^{-1} \cdot s^{-1}$ (see Table 1) are close to the theoretical ones $\mu = 1.82 \cdot 10^{-7}$ $cm^2 \cdot V^{-1} \cdot s^{-1}$ confirms the reliability of the results obtained, as well as the applicability of the method of transient electroluminescence for studying the transport of charge carriers in OLEDs based on MEH-PPV. The data obtained will be useful for finding the optimum thicknesses of the emission and buffer layers in the OLED structures, as well as for the study of transport mechanisms of charge carriers in the organic semiconductor materials under study.

This work was supported in part by the State Task (base section) of the Ministry of Education and Science of the Russian Federation (Project code 1975).

REFERENCES

1. M. Punke, S. Valouch, S. W. Kettlitz, *et al*., Lightwave Technol., **26**, No. 7, 816 (2008).
2. I. A. Barlow, T. Kreouzis, and D. G. Lidzey, Appl. Phys. Lett., **94**, 243301 (2009).
3. J. H. Burroughes, D. D.C. Bradley, A. R. Brow, *et al*., Nature, **347**, 539 (1990).
4. M. Redecker, D. D.C. Bradley, M. Inbasekaran, *et al*., Adv. Mater., **11**, No. 3, 241 (1999).
5. D. J. Pinner, R. H. Friend, and N. Tessler, J. Appl. Phys., **86**, No. 9, 5116 (1999).
6. A. V. Voitsekhovskii, A. P. Kokhanenko, and I. V. Romanov, Izv. Vyssh. Uchebn. Zaved. Fiz., **56**, No. 9/2, 109–112 (2013).
7. A. V. Voitsekhovskii, A. P. Kokhanenko, and I. V. Romanov, *et al*., Izv. Vyssh. Uchebn. Zaved. Fiz., **56**, No. 9/2, 122–124 (2013).
8. S. L. M. Mensfoort and R. Coehoorn, Phys. Rev. Lett., **100**, 086802 (2008).
9. G. G. Malliaras, J. R. Salem, P. J. Brock, and J. C. Scott, J. Appl. Phys., **84**, 1583 (1998).

10. S. L. M. Mensfoort, S. I. E. Vulto, R. A. J. Janssen, and R. Coehoorn, Phys. Rev. B, **78**, 085208 (2008).
11. I. H. Campbell, T. W. Hagler, D. L. Smith, and J. P. Ferraris, Phys. Rev. Lett., **76**, 1900 (1996).
12. C. V. Hoven, J. Peet, A. Mikhailovsky, and T. Nguyen, Appl. Phys. Lett., **94**, 033301 (2009).
13. R. J. Vries, S. L. M. Mensfoort, R. A. J. Janssen, and R. Coehoorn, Phys. Rev. B, **81**, 125203 (2010).
14. A. R. Inigo, Y. F. Huanga, J. D. Whitea, *et al*., J. Chin. Chem. Soc., **57**, No. 3B, 459 (2010).
15. Q. M. Shi, Y. B. Hou, J. Lu, *et al*., Chin. Phys. Lett., **23**, No. 4, 950 (2006).
16. H. Bassler, Phys. Status Solidi B, **175**, 15 (1993).